Correspondence

Erasure Insertion in RS-Coded SFH MFSK Subjected to Tone Jamming and Rayleigh Fading

Sohail Ahmed, Lie-Liang Yang, *Senior Member, IEEE*, and Lajos Hanzo, *Fellow, IEEE*

***Abstract*—In this paper, the achievable performance of Reed–Solomon (RS)-coded slow-frequency-hopping assisted M-ary frequency-shift keying using various erasure-insertion (EI) schemes is investigated when communicating over uncorrelated Rayleigh fading channels in the presence of multitone jamming. Three different EI schemes are considered, which are based on the output threshold test, on the ratio threshold test, and on the joint maximum output–ratio threshold test. The relevant statistics of these EI schemes are investigated mathematically, and based on these statistics, their performance is evaluated in the context of RS error-and-erasure decoding (EED). It is demonstrated that the system performance can be significantly improved by using EED, invoking the EI schemes considered.**

***Index Terms*—Error-and-erasure decoding (EED), maximum output–ratio threshold test (MO-RTT), output threshold test (OTT), ratio threshold test (RTT), slow frequency hopping (SFH), tone jamming (TJ).**

I. Introduction

In slow-frequency-hopping (SFH) systems using M-ary frequency-shift-keying (MFSK) modulation and Reed–Solomon (RS) coding, error-and-erasure decoding (EED) is typically employed for enhancing the achievable system performance when encountering interference and/or jamming. Erasure insertion (EI) is a technique which marks an RS-coded MFSK symbol as an erasure if it is deemed to be unreliable, owing to fading, interference, or jamming. It is well known that an efficient EI scheme is capable of significantly enhancing the error-correcting capability of an RS code.

Various EI schemes designed for supporting EED in conjunction with SFH MFSK using RS codes have been proposed in the literature [1]–[6], and the so-called Bayesian EI [2], [3] is capable of achieving the best bit-error-ratio (BER) performance. However, the Bayesian method requires the knowledge of all the M MFSK decision variables, and the associated complexity increases exponentially with M. When using RS coding, EI can also be achieved by attaching parity-check bits to each of the RS-coded symbols [5], [7] for checking whether the symbol was correctly received. However, this type of EI is achieved at the cost of reducing the overall throughput. Furthermore, similar to other channel-coded schemes, this type of EI degrades the achievable performance in the low-SNR region, which is due to the increased redundancy. This is because the increased redundancy reduces the transmitted energy per symbol, and as a result, the achievable uncoded error rate increases, which may therefore exceed the error-correcting capability of the RS code when the SNR is low. By contrast, the EI scheme based on ratio threshold test (RTT) [1] is a low-complexity EI scheme, which exploits the knowledge of both the maximum and the second maximum of the M decision variables of the MFSK scheme. It has been shown [1], [6], [8] that the RTT-assisted EI is capable of improving the attainable antijamming performance of SFH systems using RS coding.

In [6], two types of EI schemes have been proposed, which are based either on the output threshold test (OTT) or on the joint maximum output–ratio threshold test (MO-RTT). Like the RTT, these two EI schemes belong to the class of low-complexity EI schemes. Specifically, the OTT-based EI observes the maximum of the M decision variables, while the joint MO-RTT-based EI observes both the maximum and the second maximum of the M decision variables of the MFSK demodulator. It has been shown in [6] that the OTT-based EI is resilient against fading, while the joint MO-RTT is robust against both fading and partial-band noise jamming (PBNJ). Note that the RTT-assisted EI [1] is capable of mitigating PBNJ, but it is not particularly resilient against fading.

In this paper, we extend the results of [6] by investigating the performance of an RS-coded SFH-MFSK system when communicating over uncorrelated Rayleigh fading channels in the presence of tone jamming (TJ). In our analysis, we consider the aforementioned three types of low-complexity EI schemes, which are, respectively, derived based on the RTT, OTT, or joint MO-RTT. The decision statistics associated with these EI schemes are analyzed. With the aid of these decision statistics, a range of analytical expressions are obtained for the RS codeword error probability and the BER after EI. From our analysis and performance results, it can be shown that these EI schemes are capable of significantly improving the error performance of the SFH-MFSK systems in the presence of TJ.

The remainder of this paper is structured as follows. In Section II, the system under consideration is described, and the symbol-error rate of the uncoded SFH-MFSK system is derived. In Section III, the EI schemes considered are discussed, and the related decision statistics are investigated, while in Section IV, the numerical results are presented. Finally, in Section V, we present our conclusions.

II. System Description

The system under consideration is similar to that described in [6] and [8]. In the transmitter, the RS encoder with code rate $R_c = K/N$ converts each block of K M-ary information symbols into N coded symbols. We assume that we have $N = M - 1 = 2^b - 1$, where $b = \log_2 M$ represents the number of bits per symbol. After MFSK modulation, the frequency synthesizer, which operates under the control of a pseudonoise generator, generates a sequence of random-hopping frequencies, one of which is activated during each hop interval of duration T_h. We assume that one coded symbol is transmitted per frequency hop, and the bandwidth of one frequency-hopping (FH) tone is given by that of its main spectral lobe occupying $B = 1/T_h$.

The modulated signal of each FH tone is transmitted over a frequency-nonselective Rayleigh fading channel. We assume that fading is independent for each symbol, due to frequency diversity achieved through FH.

The transmitted signal is assumed to be interfered by a tone-jamming signal consisting of Q equal-power continuous-wave tones, each of which has a frequency equal to that of one of the M-ary signaling tones. We assume that the intentional jammer has explicit

Manuscript received February 9, 2005; revised May 25, 2006 and January 24, 2007. This work was supported in part by the Engineering and Physical Sciences Research Council, U.K., and by the European Union under the auspices of the Phoenix and Newcom Projects and by the Higher Education Commission of Pakistan. The review of this paper was coordinated by Prof. J. Shea.

The authors are with the School of Electronics and Computer Science, University of Southampton, SO1 71BJ Southampton, U.K. (e-mail: sa03r@ecs.soton.ac.uk; lly@ecs.soton.ac.uk; lh@ecs.soton.ac.uk).

Digital Object Identifier 10.1109/TVT.2007.901861

knowledge of the communication system's parameters, and thus, it is capable of adjusting the number of jamming tones accordingly, keeping the total multitone-jamming (MTJ) power fixed. We consider the case of $n = 1$-band MTJ, which is regarded as the worst-case TJ [9]. In this context, there is, at most, one interfering tone in an MFSK band, which is defined by the bandwidth occupied by the M FSK signaling tones. Furthermore, it has been shown that, for Rayleigh fading, a jammer associated with a jamming duty factor of unity inflicts the most detrimental interference upon the FH system [10]. These assumptions imply that we have $Q = N_b$, where N_b is the number of MFSK bands in the total spread-spectrum bandwidth given by $W_{\rm ss} = M \times N_b \times B$, which is assumed to be fixed. Note that the probability that a particular MFSK tone is jammed is given by $1/M$. We can define the signal-to-jammer power ratio (SJR) as [9], [11]

$$\text{SJR} = \frac{E_b}{P_{TJ}/W_{\rm ss}} = \frac{E_b}{P_J}\frac{N_b}{Q}\frac{M}{T_h} = \frac{E_s}{E_j}\frac{M}{b} \tag{1}$$

where $E_s = PT_h = bE_b$ represents the symbol energy, E_b is the energy per bit, and P is the power of the transmitted signal. Furthermore, in (1), $P_{TJ} = P_J Q$ represents the total MTJ power, P_J is the power of a single MTJ tone, and $E_j = P_J T_h$ represents the energy of a jamming-tone-per-symbol duration. Finally, we define the MTJ power spectral density as $N_j = P_{TJ}/W_{\rm ss}$ [9], [11].

In the receiver, the signal is dehopped and then demodulated by a bank of M square-law detectors. An EI device then observes all the M square-law detector outputs and either inserts an erasure, if the corresponding threshold condition is met (to be discussed in Section III), or outputs a symbol according to the standard MFSK demodulation principle. After the RS decoder has received N symbols or erasures from the EI device, it decodes them and outputs K decoded symbols with the aid of EED [6], [8]. The uninterfered signal corresponding to the ith FSK tone f_i, $i = 1, 2, \ldots, M$, at the input of the square-law detector, can be expressed as

$$r_i(t) = \alpha_s\sqrt{2PR_c}\cos\{2\pi f_i t + \phi_s\} + n_i(t) \tag{2}$$

where α_s represents the amplitude attenuation factor due to Rayleigh fading and ϕ_s includes all the phases in the received signal due to FH, carrier modulation, and MFSK modulation, as well as that induced by the fading channel. Finally, $n_i(t)$ represents the AWGN having zero mean and double-sided power spectral density of $N_0/2$.

Assuming that the first FSK tone is activated, let us denote the output of the square-law detector corresponding to the signal tone by U_1 when it is uninterfered and by $U_{1(j)}$ when the frequency of the interfering tone coincides with that of the signal tone. Similarly, let U_i and $U_{i(j)}$ denote the corresponding unjammed and jammed outputs of the square-law detector corresponding to the ith nonsignal tone. Assuming independent Rayleigh fading of the desired signal and the jamming tones, it can be shown that the outputs of the square-law detectors are given by [9], [12]

$$U_{1(j)} = \left|\alpha_s\sqrt{R_cE_s}e^{j\phi_s} + \alpha_j\sqrt{E_j}e^{j\phi_j} + n_1\right|^2 \tag{3}$$

$$U_1 = \left|\alpha_s\sqrt{R_cE_s}e^{j\phi_s} + n_1\right|^2 \tag{4}$$

$$U_{i(j)} = \left|\alpha_j\sqrt{E_j}e^{j\phi_j} + n_i\right|^2, \qquad i = 2, 3, \ldots, M \tag{5}$$

and

$$U_i = |n_i|^2, \qquad i = 2, 3, \ldots, M \tag{6}$$

where α_j and ϕ_j are the amplitude attenuation factor and the phase associated with the interference tone, respectively. It is shown in (3)–(5) that all the square-law detector outputs are central Chi-squared distributed with double degrees of freedom or exponentially distributed [12]. Thus, it can be shown that the probability density function (pdf) of the noise-normalized square-law detector output may be expressed as

$$f_{U_{1(j)}}(y) = \frac{1}{1+\gamma_{c(j)}}\exp\left[-\frac{y}{1+\gamma_{c(j)}}\right], \qquad y \geq 0 \tag{7}$$

$$f_{U_1}(y) = \frac{1}{1+\gamma_c}\exp\left[-\frac{y}{1+\gamma_c}\right], \qquad y \geq 0 \tag{8}$$

$$f_{U_{i(j)}}(y) = \frac{1}{1+\gamma_j}\exp\left[-\frac{y}{1+\gamma_j}\right], \qquad y \geq 0,\ i > 1 \tag{9}$$

and

$$f_{U_i}(y) = \exp(-y), \qquad y \geq 0,\ i > 1 \tag{10}$$

where $\gamma_c = \Omega_s R_c E_s/N_0$, $\gamma_j = \Omega_j E_j/N_0$, and $\gamma_{c(j)} = \gamma_c + \gamma_j$. Moreover, $\Omega_s = E[\alpha_s^2]$ and $\Omega_j = E[\alpha_j^2]$.

Let H_1 represent the hypothesis that the transmitted symbol is correctly detected, and H_0 denote the hypothesis that the transmitted symbol is incorrectly detected, when using hard decisions. It can be shown that the probability $P(H_1)$ of a correct decision for the uncoded system is given by

$$\begin{aligned}P(H_1) &= \frac{1}{M}\int_0^\infty f_{U_{1(j)}}(y)\left[\int_0^y f_{U_i}(x)dx\right]^{M-1}dy \\ &\quad + \left(\frac{M-1}{M}\right)\int_0^\infty f_{U_1}(y)\int_0^y f_{U_{i(j)}}(x)dx\left[\int_0^y f_{U_i}(x)dx\right]^{M-2}dy \\ &= \frac{1}{M}\sum_{n=0}^{M-1}(-1)^n\binom{M-1}{n}\frac{1}{1+n\left(1+\gamma_{c(j)}\right)} \\ &\quad + \left(\frac{M-1}{M}\right)\sum_{n=0}^{M-2}(-1)^n\binom{M-2}{n} \\ &\quad \times\left[\frac{1}{1+n(1+\gamma_c)} - \frac{1+\gamma_j}{2+\gamma_c+\gamma_j+n(1+\gamma_c)(1+\gamma_j)}\right].\end{aligned} \tag{11}$$

Thus, the probability of an incorrect hard decision is expressed as $P(H_0) = 1 - P(H_1)$.

III. Error Probability of RS-Coded System Using EED

Let us now investigate the achievable performance of the SFH-MFSK system when EED is considered. We choose three different EI schemes, each of which may be employed for inserting an erasure after energy detection on the basis of a certain test condition. Let $Y_1 = \max[U_1, U_2, \ldots, U_M]$ and $Y_2 = \max_2[U_1, U_2, \ldots, U_M]$ denote the maximum and second maximum of the square-law detector outputs, respectively. In the context of the OTT, if $Y_1 \leq Y_T$ is satisfied,

where Y_T is a preset threshold, the associated demodulated symbol should be erased. Otherwise, if we have $Y_1 > Y_T$, the demodulator outputs an RS code symbol [6]. By contrast, in the context of the RTT, a preset threshold λ_T can be invoked, in order to erase the low-reliability symbols, whenever we have $Y_2/Y_1 \geq \lambda_T$ [1], [6]. Finally, in the context of the joint MO-RTT [6], we assume that Y_T and λ_T are two thresholds, which activate an EI, whenever we have $Y_1 \leq Y_T$ and $Y_2/Y_1 \geq \lambda_T$.

Next, we determine the expressions for the pdfs of Y_1 in the context of the OTT of $\lambda = Y_2/Y_1$ in the context of the RTT, as well as the joint pdf of Y_1 and $\lambda = Y_2/Y_1$ in the context of the MO-RTT. The pdf of Y_1, conditioned on the correct decision hypothesis of H_1, can be expressed as follows:

$$\begin{aligned}
&f_{Y_1}(y_1|H_1) \\
&\quad = \frac{d}{dy_1} P[Y_1 \leq y_1|H_1] \\
&\quad = \frac{1}{P(H_1)} \frac{d}{dy_1} P[Y_1 \leq y_1, H_1] \\
&\quad = \frac{1}{P(H_1)} \frac{d}{dy_1} \\
&\qquad \left[\frac{1}{M} P\left[U_{1(j)} = Y_1 \leq y_1, \left(U_i \leq U_{1(j)}\right)_{i=2}^{M} \right] + \left(1 - \frac{1}{M}\right) \right. \\
&\qquad\quad \left. \times P\left[U_1 = Y_1 \leq y_1, U_{i(j)} \leq U_1, (U_i \leq U_1)_{i=2, i(j)\neq i}^{M} \right] \right] \\
&\quad = \frac{1}{P(H_1)} \frac{d}{dy_1} \left[\frac{1}{M} \int_0^{y_1} f_{U_{1(j)}}(x) dx \left[\int_0^x f_{U_i}(y) dy \right]^{M-1} \right. \\
&\qquad\qquad + \left(1 - \frac{1}{M}\right) \int_0^{y_1} f_{U_1}(x) dx \left[\int_0^x f_{U_{i(j)}}(y) dy \right] \\
&\qquad\qquad \left. \times \left[\int_0^x f_{U_i}(y) dy \right]^{M-2} \right] \qquad (12)
\end{aligned}$$

where $P[\cdot]$ denotes the probability of an event. Upon substituting the corresponding pdfs from (7)–(10) into the above equation, the pdf of Y_1 can be expressed as

$$\begin{aligned}
f_{Y_1}(y_1|H_1) &= \frac{1}{P(H_1)} \frac{1}{M} \\
&\quad \times \left[\frac{1}{1+\gamma_{c(j)}} \exp\left(\frac{-y_1}{1+\gamma_{c(j)}} \right) \times (1 - e^{-y_1})^{M-1} \right. \\
&\quad + (M-1) \frac{1}{1+\gamma_c} \exp\left(\frac{-y_1}{1+\gamma_c} \right) \\
&\quad \left. \times (1 - e^{-y_1})^{M-2} \left[1 - \exp\left(\frac{-y_1}{1+\gamma_j} \right) \right] \right] \qquad (13)
\end{aligned}$$

where $P(H_1)$ is given by (11).When deriving the pdf $f_{Y_1}(y_1|H_0)$, we should consider the fact that, if a nonsignal tone is jammed, the largest of the square-law detector outputs, i.e., Y_1, may correspond to either the jammed nonsignal tone or to one of the unjammed nonsignal tones. Hence, we have

$$\begin{aligned}
f_{Y_1}(y_1|H_0) &= \frac{d}{dy_1} P[Y_1 \leq y_1|H_0] \\
&= \frac{1}{P(H_0)} \frac{d}{dy_1} P[Y_1 \leq y_1, H_0] \\
&= \frac{1}{P(H_0)} \frac{d}{dy_1} \\
&\quad \left[\frac{1}{M}(M-1) P\left[U_i = Y_1 \leq y_1, U_{1(j)} \leq U_i, \right. \right. \\
&\qquad \left. \left. (U_j \leq U_i)_{j=3, j\neq i}^{M} \right] + \left(\frac{M-1}{M} \right) \right. \\
&\qquad \times \left\{ (M-2) P\left[U_i = Y_1 \leq y_1, U_1 \leq U_i, \right. \right. \\
&\qquad\qquad \left. U_{i(j)} \leq U_i, (U_j \leq U_{i(j)})_{j=4, j\neq i}^{M} \right] \\
&\qquad\qquad + P\left[U_{i(j)} = Y_1 \leq y_1, U_1 \leq U_{i(j)} \right. \\
&\qquad\qquad \left. \left. \left(U_j \leq U_{i(j)} \right)_{j=2, j\neq i(j)}^{M} \right] \right\} \Bigg] \\
&= \frac{1}{P(H_0)} \frac{d}{dy_1} \\
&\quad \times \left[\frac{1}{M}(M-1) \int_0^{y_1} f_{U_i}(x) dx \left[\int_0^x f_{U_{1(j)}}(y) dy \right] \right. \\
&\qquad \times \left[\int_0^x f_{U_i}(y) dy \right]^{M-2} + \left(\frac{M-1}{M} \right) \\
&\qquad \times \left\{ (M-2) \int_0^{y_1} f_{U_i}(x) dx \left[\int_0^x f_{U_1}(y) dy \right] \right. \\
&\qquad\quad \times \left[\int_0^x f_{U_{i(j)}}(y) dy \right] \left[\int_0^x f_{U_i}(y) dy \right]^{M-3} \\
&\qquad\quad + \int_0^{y_1} f_{U_{i(j)}}(x) dx \left[\int_0^x f_{U_1}(y) dy \right] \\
&\qquad\quad \left. \left. \times \left[\int_0^x f_{U_i}(y) dy \right]^{M-2} \right\} \right] \\
&= \frac{1}{P(H_0)} \left(\frac{M-1}{M} \right) \\
&\quad \times \left[\left[1 - \exp\left(\frac{-y_1}{1+\gamma_{c(j)}} \right) \right] \right. \\
&\qquad \times \left(1 - e^{-y_1} \right)^{M-2} e^{-y_1} + \left[1 - \exp\left(\frac{-y_1}{1+\gamma_c} \right) \right] \\
&\qquad \times \left\{ (M-2) e^{-y_1} (1 - e^{-y_1})^{M-3} \right. \\
&\qquad\quad \times \left[1 - \exp\left(\frac{-y_1}{1+\gamma_j} \right) \right] + \frac{1}{1+\gamma_j} \\
&\qquad\quad \left. \left. \times \exp\left(\frac{-y_1}{1+\gamma_j} \right) (1 - e^{-y_1})^{M-2} \right\} \right]. \qquad (14)
\end{aligned}$$

The joint pdf of Y_1 and Y_2, which is conditioned on the hypothesis H_1, can be expressed as

$$
\begin{aligned}
&f_{Y_1,Y_2}(y_1,y_2|H_1)\\
&\quad=\frac{\partial^2}{\partial y_1\partial y_2}P[Y_1\le y_1,Y_2\le y_2|H_1]\\
&\quad=\frac{1}{P(H_1)}\frac{\partial^2}{\partial y_1\partial y_2}P[Y_1\le y_1,Y_2\le y_2,H_1]\\
&\quad=\frac{1}{P(H_1)}\frac{\partial^2}{\partial y_1\partial y_2}\\
&\qquad\left[\frac{M-1}{M}\int_0^{y_2}f_{U_i}(x)dx\left[\int_x^{y_1}f_{U_{1(j)}}(y)dy\right]\right.\\
&\qquad\quad\times\left[\int_0^{x}f_{U_i}(y)dy\right]^{M-2}+\frac{M-1}{M}\\
&\qquad\quad\times\left\{(M-2)\int_0^{y_2}f_{U_i}(x)dx\left[\int_x^{y_1}f_{U_1}(y)dy\right]\right.\\
&\qquad\qquad\times\left[\int_0^{x}f_{U_{i(j)}}(y)dy\right]\left[\int_0^{x}f_{U_i}(y)dy\right]^{M-3}\\
&\qquad\qquad+\int_0^{y_2}f_{U_{i(j)}}(x)dx\left[\int_x^{y_1}f_{U_1}(y)dy\right]\\
&\qquad\qquad\left.\left.\times\left[\int_0^{x}f_{U_i}(y)dy\right]^{M-2}\right\}\right]\\
&\quad=\frac{1}{P(H_1)}\left(\frac{M-1}{M}\right)\\
&\qquad\times\left[f_{U_{1(j)}}(y_1)f_{U_i}(y_2)\left[\int_0^{y_2}f_{U_i}(y)dy\right]^{M-2}+f_{U_1}(y_1)\right.\\
&\qquad\quad\times\left\{(M-2)\int_0^{y_2}f_{U_{i(j)}}(y)dy\left[\int_0^{y_2}f_{U_i}(y)dy\right]^{M-3}\right.\\
&\qquad\qquad\left.\left.\times f_{U_i}(y_2)+f_{U_{i(j)}}(y_2)\left[\int_0^{y_2}f_{U_i}(y)dy\right]^{M-2}\right\}\right].
\end{aligned}
\tag{15}
$$

Now, let $Y=Y_1$ and $\lambda=Y_2/Y_1$. Then, upon using the expressions for the corresponding pdfs, it can be shown that the joint pdf of Y and λ, which is the pdf associated with the MO-RTT-based EI scheme, which is conditioned on the hypothesis H_1, can be expressed as [6], [12]

$$
\begin{aligned}
&f_{Y,\lambda}(y,r|H_1)\\
&\quad=\left(\frac{M-1}{M}\right)\frac{y}{P(H_1)}\\
&\qquad\times\left[\frac{1}{1+\gamma_{c(j)}}e^{-yr}\exp\left(\frac{-y}{1+\gamma_{c(j)}}\right)(1-e^{-yr})^{M-2}\right.\\
&\qquad\quad+\frac{1}{1+\gamma_c}\exp\left(\frac{-y}{1+\gamma_c}\right)\\
&\qquad\quad\times\left\{(M-2)e^{-yr}\left[1-\exp\left(\frac{-yr}{1+\gamma_j}\right)\right](1-e^{-yr})^{M-3}\right.\\
&\qquad\qquad\left.\left.+\frac{1}{1+\gamma_j}\exp\left(\frac{-yr}{1+\gamma_j}\right)(1-e^{-yr})^{M-2}\right\}\right].
\end{aligned}
\tag{16}
$$

The joint pdf of Y_1 and Y_2, which is conditioned on the hypothesis H_0, can be expressed as

$$
\begin{aligned}
&f_{Y_1,Y_2}(y_1,y_2|H_0)\\
&\quad=\frac{\partial^2}{\partial y_1\partial y_2}P[Y_1\le y_1,Y_2\le y_2|H_0]\\
&\quad=\frac{1}{P(H_0)}\frac{\partial^2}{\partial y_1\partial y_2}P[Y_1\le y_1,Y_2\le y_2,H_0]\\
&\quad=\frac{1}{P(H_0)}\frac{\partial^2}{\partial y_1\partial y_2}\\
&\qquad\left[\frac{1}{M}(M-1)\left\{\int_0^{y_2}f_{U_{1(j)}}(x)dx\left[\int_x^{y_1}f_{U_i}(y)dy\right]\right.\right.\\
&\qquad\qquad\times\left[\int_0^{x}f_{U_i}(y)dy\right]^{M-2}+(M-2)\\
&\qquad\qquad\times\int_0^{y_2}f_{U_i}(x)dx\left[\int_x^{y_1}f_{U_i}(y)dy\right]\\
&\qquad\qquad\left.\left.\times\left[\int_0^{x}f_{U_{1(j)}}(y)dy\right]\left[\int_0^{x}f_{U_i}(y)dy\right]^{M-3}\right\}\right.\\
&\qquad+\left(\frac{M-1}{M}\right)\left\{\int_0^{y_2}f_{U_1}(x)dx\left\{\left[\int_x^{y_1}f_{U_{i(j)}}(y)dy\right]\right.\right.\\
&\qquad\qquad\times\left[\int_0^{x}f_{U_i}(y)dy\right]^{M-2}+(M-2)\\
&\qquad\qquad\times\left[\int_x^{y_1}f_{U_i}(y)dy\right]\left[\int_0^{x}f_{U_{i(j)}}(y)dy\right]\\
&\qquad\qquad\left.\left.\left.\times\left[\int_0^{x}f_{U_i}(y)dy\right]^{M-3}\right\}\right\}\right].
\end{aligned}
$$

$$
\begin{aligned}
&+(M-2)\int_0^{y_2} f_{U_i}(x)dx \\
&\times\left[\int_x^{y_1} f_{U_{i(j)}}(y)dy\right]\left[\int_0^{x} f_{U_1}(y)dy\right] \\
&\times\left[\int_0^{x} f_{U_i}(y)dy\right]^{M-3} + (M-2) \\
&\times\int_0^{y_2} f_{U_{i(j)}}(x)dx\left[\int_x^{y_1} f_{U_i}(y)dy\right] \\
&\times\left[\int_0^{x} f_{U_1}(y)dy\right]\left[\int_0^{x} f_{U_i}(y)dy\right]^{M-3} \\
&+(M-3)\int_0^{y_2} f_{U_i}(x)dx\left[\int_x^{y_1} f_{U_i}(y)dy\right] \\
&\times\left[\int_0^{x} f_{U_{i(j)}}(y)dy\right]\left[\int_0^{x} f_{U_1}(y)dy\right] \\
&\times\left[\int_0^{x} f_{U_i}(y)dy\right]^{M-4}\Bigg\}\Bigg]. \qquad (17)
\end{aligned}
$$

After partial differentiation, the above equation can be written as

$$
\begin{aligned}
&f_{Y_1,Y_2}(y_1,y_2|H_0) \\
&=\frac{1}{P(H_0)}\left(\frac{M-1}{M}\right) \\
&\times\left[f_{U_{1(j)}}(y_2)f_{U_i}(y_1)\left[\int_0^{y_2} f_{U_i}(y)dy\right]^{M-2}\right. \\
&+(M-2)f_{U_i}(y_2)f_{U_i}(y_1)\int_0^{y_2} f_{U_{1(j)}}(y)dy \\
&\times\left[\int_0^{y_2} f_{U_i}(y)dy\right]^{M-3} + f_{U_1}(y_2)f_{U_{i(j)}}(y_1) \\
&\times\left[\int_0^{y_2} f_{U_i}(y)dy\right]^{M-2} + (M-2)f_{U_1}(y_2)f_{U_i}(y_1) \\
&\times\int_0^{y_2} f_{U_{i(j)}}(y)dy\left[\int_0^{y_2} f_{U_i}(y)dy\right]^{M-3} \\
&+(M-2)f_{U_i}(y_2)f_{U_{i(j)}}(y_1)\int_0^{y_2} f_{U_1}(y)dy \\
&\times\left[\int_0^{y_2} f_{U_i}(y)dy\right]^{M-3} + (M-2)f_{U_i}(y_1)\int_0^{y_2} f_{U_1}(y)dy \\
&\times\left\{f_{U_{i(j)}}(y_2)\left[\int_0^{y_2} f_{U_i}(y)dy\right]^{M-3} + (M-3)f_{U_i}(y_2)\right. \\
&\left.\left.\times\int_0^{y_2} f_{U_{i(j)}}(y)dy\left[\int_0^{y_2} f_{U_i}(y)dy\right]^{M-4}\right\}\right]. \qquad (18)
\end{aligned}
$$

After changing the variables from Y_1 and Y_2 to Y and $\lambda = Y_2/Y_1$ [6], [12], [13], we obtain the corresponding joint pdf, which is conditioned on the hypothesis H_0, which is given in (19), shown at the bottom of the page.

$$
\begin{aligned}
f_{Y,\lambda}(y,r|H_0) = &\left(\frac{M-1}{M}\right) y\frac{1}{P(H_0)}\left[e^{-y}\frac{1}{1+\gamma_{c(j)}}\exp\left(\frac{-yr}{1+\gamma_{c(j)}}\right)(1-e^{-yr})^{M-2} + (M-2)e^{-y(r+1)}\left[1-\exp\left(\frac{-yr}{1+\gamma_{c(j)}}\right)\right](1-e^{-yr})^{M-3}\right. \\
&+\frac{1}{1+\gamma_c}\exp\left(\frac{-yr}{1+\gamma_c}\right)\left\{\frac{1}{1+\gamma_j}\exp\left(\frac{-y}{1+\gamma_j}\right)(1-e^{-yr})^{M-2}\right. \\
&\left.+(M-2)e^{-y}\left[1-\exp\left(\frac{-yr}{1+\gamma_j}\right)\right](1-e^{-yr})^{M-3}\right\} \\
&+(M-2)\left[1-\exp\left(\frac{-yr}{1+\gamma_c}\right)\right]\left\{(1-e^{-yr})^{M-3}\frac{1}{1+\gamma_j}\exp\left(\frac{-y}{1+\gamma_j}\right)e^{-yr}\right. \\
&+e^{-y}\frac{1}{1+\gamma_j}\exp\left(\frac{-yr}{1+\gamma_j}\right)(1-e^{-yr})^{M-3} \\
&\left.\left.+(M-3)e^{-y(r+1)}(1-e^{-yr})^{M-4}\left[1-\exp\left(\frac{-yr}{1+\gamma_j}\right)\right]\right\}\right] \qquad (19)
\end{aligned}
$$

Finally, we derive the pdfs corresponding to the ratio $\lambda = Y_2/Y_1$ in the context of the RTT-assisted EI scheme. These pdfs can be readily obtained from (16) and (19) by integrating them in terms of Y from 0 to ∞, yielding the expressions given in (20) and (21), shown at the bottom of the page.

From the pdfs derived above, it is straightforward to express the probability P_e of erasure and probability P_t of error after erasure for a chosen threshold corresponding to a certain EI scheme. The required expressions have been given in [6]. Consequently, the probability of not decoding the codeword correctly, i.e., the codeword error probability P_w, can be expressed as [6]

$$P_w = \sum_{i=0}^{N} \sum_{j=j_0(i)}^{N-i} \binom{N}{i} \binom{N-i}{j} (P_t)^i (P_e)^j (1-P_t-P_e)^{N-i-j} \tag{22}$$

$$f_\lambda(r|H_1) = \int_0^\infty f_{Y,\lambda}(y,r|H_1)dy$$

$$= \left(\frac{M-1}{M}\right) \frac{1}{P(H_1)} \left[\sum_{n=0}^{M-2} (-1)^n \binom{M-2}{n} \left\{ \frac{1+\gamma_{c(j)}}{\left[1+r(n+1)\left(1+\gamma_{c(j)}\right)\right]^2} + \frac{(1+\gamma_c)(1+\gamma_j)}{\left[1+\gamma_j+r(1+\gamma_c)\left\{1+n(1+\gamma_j)\right\}\right]^2} \right\} \right.$$

$$\left. + (M-2) \sum_{n=0}^{M-3} (-1)^n \binom{M-3}{n} \left\{ \frac{1+\gamma_c}{[1+r(n+1)(1+\gamma_c)]^2} - \frac{(1+\gamma_c)(1+\gamma_j)^2}{\left[1+\gamma_j+r(1+\gamma_c)\{1+(n+1)(1+\gamma_j)\}\right]^2} \right\} \right] \tag{20}$$

$$f_\lambda(r|H_0) = \int_0^\infty f_{Y,\lambda}(y,r|H_0)dy$$

$$= \left(\frac{M-1}{M}\right) \frac{1}{P(H_0)} \left[\sum_{n=0}^{M-2} (-1)^n \binom{M-2}{n} \left\{ \frac{1+\gamma_{c(j)}}{\left[r+(nr+1)\left(1+\gamma_{c(j)}\right)\right]^2} + \frac{(1+\gamma_c)(1+\gamma_j)}{\left[1+\gamma_c+r(1+\gamma_j)\left\{1+n(1+\gamma_c)\right\}\right]^2} \right\} \right.$$

$$+ (M-2) \sum_{n=0}^{M-3} (-1)^n \binom{M-3}{n} \left\{ \frac{1}{[1+r(n+1)]^2} - \frac{\left(1+\gamma_{c(j)}\right)^2}{\left[r+\{1+r(n+1)\}\left(1+\gamma_{c(j)}\right)\right]^2} \right.$$

$$+ \frac{1+\gamma_c}{[r+(rn+1)(1+\gamma_c)]^2} + \frac{1+\gamma_j}{[r+(rn+1)(1+\gamma_j)]^2}$$

$$- \frac{(1+\gamma_c)(1+\gamma_j)(2+\gamma_c+\gamma_j)}{[(1+nr)(1+\gamma_c)(1+\gamma_j)+r(2+\gamma_c+\gamma_j)]^2}$$

$$+ \frac{1+\gamma_j}{[1+r(n+1)(1+\gamma_j)]^2}$$

$$\left. - \frac{(1+\gamma_c)^2(1+\gamma_j)}{\left[1+\gamma_c+r(1+\gamma_j)\{1+(n+1)(1+\gamma_c)\}\right]^2} \right\}$$

$$+ (M-2)(M-3) \sum_{n=0}^{M-4} (-1)^n \binom{M-4}{n} \left\{ \frac{1}{[1+r(n+1)]^2} - \frac{(1+\gamma_c)^2}{\left[r+\{1+r(n+1)\}(1+\gamma_c)\right]^2} \right.$$

$$+ \frac{(1+\gamma_c)^2(1+\gamma_j)^2}{\left[\{1+r(n+1)\}(1+\gamma_c)(1+\gamma_j)+r(2+\gamma_c+\gamma_j)\right]^2}$$

$$\left. \left. - \frac{(1+\gamma_j)^2}{\left[r+\{1+r(n+1)\}(1+\gamma_j)\right]^2} \right\} \right] \tag{21}$$

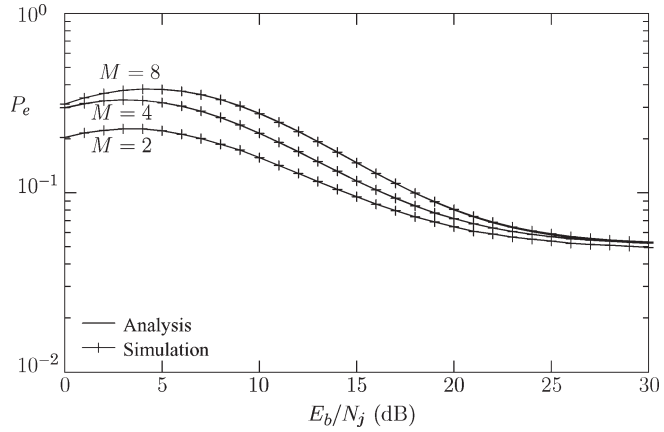

Fig. 1. Analytical and simulation results for the probability of erasure corresponding to the RTT plotted against E_b/N_j when the uncoded SFH-MFSK system is subjected to Rayleigh fading and $n = 1$-band MTJ and when assuming $\lambda_T = 0.4$ and $E_b/N_0 = 16$ dB.

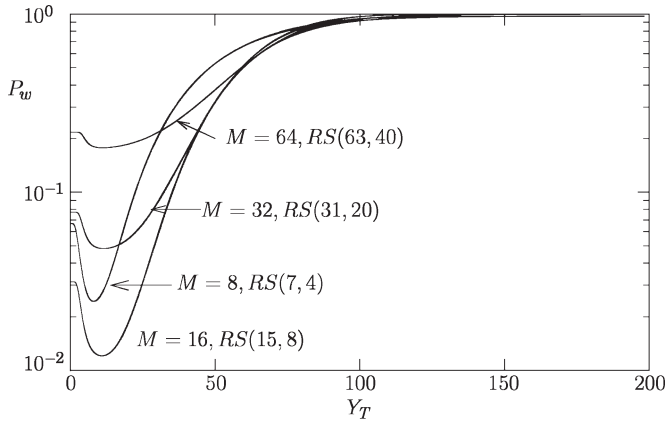

Fig. 2. Codeword error probability versus threshold Y_T for RS-coded SFH MFSK using the OTT when subjected to Rayleigh fading and $n = 1$-band MTJ at $E_b/N_j = 20$ dB, $E_b/N_0 = 16$ dB, and various values of M.

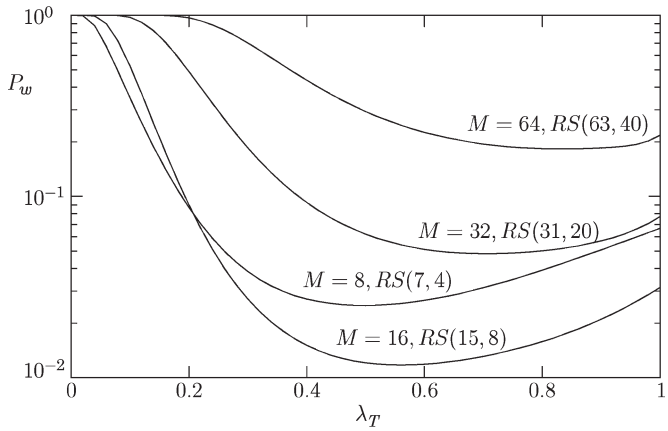

Fig. 3. Codeword error probability versus threshold λ_T for RS-coded SFH MFSK using the RTT when subjected to Rayleigh fading and $n = 1$-band MTJ at $E_b/N_j = 20$ dB, $E_b/N_0 = 16$ dB, and various values of M.

where we have $j_0(i) = \max\{0, N - K + 1 - 2i\}$. The symbol-error rate after EED can be expressed as [14]

$$P_s \approx \frac{1}{N} \sum_{i=0}^{N} \sum_{j=j_0(i)}^{N-i} (i+j) \binom{N}{i} \binom{N-i}{j} \times (P_t)^i (P_e)^j (1 - P_t - P_e)^{N-i-j}. \quad (23)$$

The BER of the SFH-MFSK system employing RS EED can be determined from the symbol-error rate given by (23) using the expression $P_b = P_s((M/2)/(M-1))$ [12].

IV. Analytical Results and Discussion

Based on the BER derived for the RS-coded system employing one of the three EI schemes considered, we are now capable of studying the properties of the system. In Fig. 1, the probability of erasure corresponding to $\lambda_T = 0.4$ in the context of the RTT has been shown based on both analytical and simulation results when the SFH-MFSK system communicates in a Rayleigh fading channel and is interfered by $n = 1$-band MTJ. The results shown in Fig. 1 are for $M = 2$, 4, and 8 and indicate that our analysis of the probability of erasure is correct.

In Figs. 2 and 3, we evaluated the codeword error probability against a range of Y_T and λ_T values, respectively, as well as for various values of M and the corresponding RS codes. We observe that, for each value of M, an optimum threshold value exists in the context of both the OTT and the RTT, corresponding to the minimum system codeword error probability that is achieved. In a similar fashion, it can be shown that, in the context of the MO-RTT, there exist optimum values of the thresholds of λ_T and Y_T, which result in the best system performance when employing EED.

We also observe in Figs. 2 and 3 that the system using $M = 16$ achieves the lowest codeword error probability in both figures. This observation can be explained as follows. It is well known that the performance of the MFSK system recorded in the absence of interference improves as M increases, which is a benefit of increased symbol energy [12], whereas the detrimental effects of single TJ imposed on the performance of FH-MFSK become more severe as M is increased [9]. Moreover, in the context of the RS-coded system, using a higher value of M implies that the RS code operates over a larger Galois field and, hence, potentially becomes capable of correcting more bits per symbol, although the number of symbol errors corrected remains $t = (N - K)/2$ when the code rate is fixed to K/N [12]. Thus, in the context of the system under consideration, increasing the value of M results in conflicting trends. More specifically, a high value of M results in an increased symbol energy and a potentially higher error-correcting capability, but it also leads to higher susceptibility to single-tone interference. These contrasting effects of increasing the value of M imply that there exists an optimum M value, which achieves the best error performance. Consequently, we observe that, corresponding to the system parameters assumed in Figs. 2 and 3, the system corresponding to $M = 16$ achieves the best performance when using RS EED.

In Fig. 4, we evaluated the BER of RS-coded SFH MFSK when it employs OTT-based EI and when assuming optimum threshold values for each value of E_b/N_j and M. The results of Fig. 4 show that EED outperforms the "error-correcting only" decoding for all values of M. However, the BER improvement of EED portrayed in Fig. 3 is noteworthy only when the jammer power is sufficiently low. Furthermore, when the SJR is sufficiently high, i.e., when E_b/N_j exceeds 20 dB, a higher performance gain can be achieved, particularly in the case of $M = 32$, owing to the higher error-correcting capability of the RS(31,20) code used. Finally, in Fig. 5, we show our BER performance comparison for the RS-coded SFH-MFSK system when employing the three different types of EI schemes considered. We can see that the BERs of the three types of EI schemes are hardly

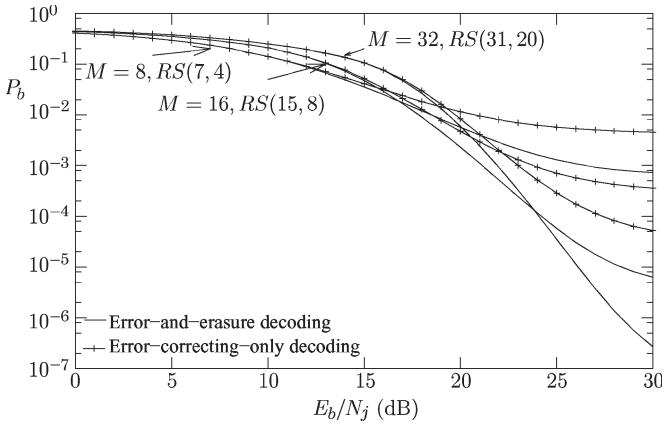

Fig. 4. BER versus E_b/N_j performance of RS-coded SFH MFSK using the OTT-based EI for $E_b/N_0 = 16$ dB when subjected to Rayleigh fading and $n = 1$-band MTJ and assuming optimum thresholds.

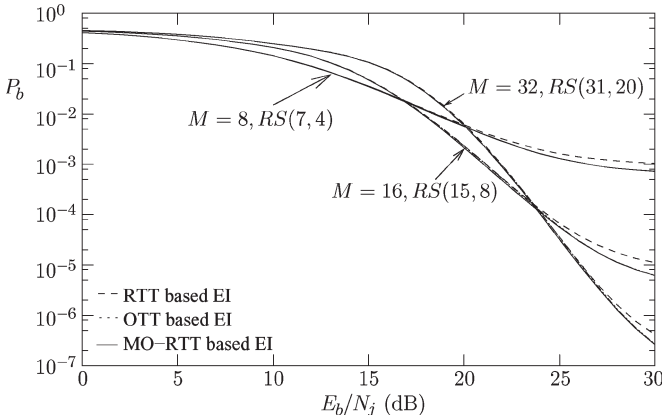

Fig. 5. Comparison of the BER versus E_b/N_j performance of the RS-coded SFH-MFSK system using OTT-, RTT-, and MO-RTT-based EI for $E_b/N_0 = 16$ dB when subjected to Rayleigh fading and $n = 1$-band MTJ and when assuming optimum thresholds.

distinguishable from each other when E_b/N_j is relatively low, i.e., when $E_b/N_j \leq 20$ dB. By contrast, when E_b/N_j is sufficiently high, i.e., when $E_b/N_j \geq 25$ dB, both the OTT and the MO-RTT outperform the RTT. It can be inferred from the definition of the EI schemes outlined in Section III that the OTT-based scheme provides a technique for erasing symbols that suffer from strong fading while the RTT-based method seeks to eliminate symbols that are rendered unreliable owing to interference. Consequently, when the jamming power is low, most errors occur due to Rayleigh fading, and the OTT-based EI outperforms the RTT-based scheme, as shown in Fig. 5. Finally, the MO-RTT-based EI performs slightly better than both the OTT- and RTT-based EI, since it makes use of the combined information based on the OTT and the RTT. However, for the system under consideration, the BER performance of the MO-RTT is close to that of the OTT. In order to show the slight differences in detail, the minimum achievable BER values of SFH 16-ary FSK have been summarized in Table I when invoking the RTT-, the OTT-, and the MO-RTT-based EI schemes. It is noteworthy from the results shown in Table I that, when E_b/N_j is relatively low, i.e., 15 or 20 dB, and E_b/N_0 is high, i.e., 20 or 25 dB, the RTT outperforms the OTT. For all other values of E_b/N_j and E_b/N_0 shown in Table I, the OTT performs better than the RTT-based EI scheme. This observation implies that, when the thermal noise power is high, the OTT-based scheme is more effective than the RTT-based scheme.

TABLE I
COMPARISON OF BER ACHIEVED BY RS-CODED SFH 16-ARY FSK USING VARIOUS EI SCHEMES, WHEN SUBJECTED TO RAYLEIGH FADING AND $n = 1$-BAND MTJ

E_b/N_j (dB)	E_b/N_0 (dB)	Minimum BER		
		RTT	OTT	MO-RTT
15	5	0.196845	0.19082	0.19082
	10	0.0794641	0.07266	0.07259
	15	0.0503719	0.048873	0.048778
	20	0.0444911	0.045427	0.04432
	25	0.043019	0.04448	0.043019
20	5	0.1682	0.16022	0.16005
	10	0.01828	0.014816	0.014718
	15	0.0028153	0.0026626	0.0025726
	20	0.0016041	0.0017065	0.0015004
	25	0.0013616	0.0014783	0.0012826
25	5	0.1618	0.15215	0.15193
	10	0.0089072	0.0064891	0.0064363
	15	0.00012875	0.00010024	9.8246e-5
	20	1.6447e-5	1.5894e-5	1.2825e-5
	25	1.1437e-5	9.2379e-6	7.3238e-6
30	5	0.16093	0.15022	0.14999
	10	0.00759135	0.0053956	0.0053506
	15	3.55648e-5	2.0125e-5	1.9863e-5
	20	2.11812e-7	1.7064e-7	1.6061e-7
	25	3.63849e-8	2.6517e-8	1.9652e-8

V. CONCLUSION

In this contribution, we have analyzed the BER performance of the RS-coded SFH-MFSK system using EI when the SFH-MFSK signals are transmitted over Rayleigh fading channels in the presence of $n = 1$-band MTJ. We found that, with the aid of RS EED assisted by one of the three EI schemes considered in this contribution, the system performance may be significantly improved, provided that the jamming power is not excessively high. It was demonstrated that, when the jamming power is low, the OTT outperforms the RTT. Since the MO-RTT is constituted by an amalgam of the OTT- and RTT-based EI schemes, it either outperforms both the OTT and the RTT or results in a performance which matches the better of the other two. However, the corresponding performance is typically close to that of one of its counterparts. The results also showed that, in general, when the SFH-MFSK system experiences TJ, there is an optimum value of M, which results in the best performance.

REFERENCES

[1] A. J. Viterbi, "A robust ratio-threshold technique to mitigate tone and partial band jamming in coded MFSK systems," in *IEEE Mil. Commun. Conf. Rec.*, Oct. 1982, pp. 22.4.1–22.4.5.

[2] C. W. Baum and M. B. Pursley, "Bayesian methods of erasure insertion in frequency-hop communication with partial-band interference," *IEEE Trans. Commun.*, vol. 40, no. 7, pp. 1231–1238, Jul. 1992.

[3] C. W. Baum and M. B. Pursley, "Erasure insertion in frequency-hop communications with fading and partial-band interference," *IEEE Trans. Veh. Technol.*, vol. 46, no. 4, pp. 949–956, Nov. 1997.

[4] T. G. Macdonald and M. B. Pursley, "Staggered interleaving and iterative errors-and-erasures decoding for frequency-hop packet radio," *IEEE Trans. Wireless Commun.*, vol. 2, no. 1, pp. 92–98, Jan. 2003.

[5] M. B. Pursley and C. S. Wilkins, "An investigation of relationships between side information and information rate in slow-frequency-hop communications," in *Proc. IEEE MILCOM Conf.*, Nov. 1997, vol. 2, pp. 545–549.

[6] L. L. Yang and L. Hanzo, "Low complexity erasure insertion in RS-coded SFH spread-spectrum communications with partial-band interference and Nakagami-m fading," *IEEE Trans. Commun.*, vol. 50, no. 6, pp. 914–925, Jun. 2002.

[7] M. B. Pursley and C. S. Wilkins, "A comparison of two methods for erasure generation in frequency-hop communications with partial-band interference and Rayleigh fading," in *Proc. IEEE MILCOM Conf.*, Oct. 1996, vol. 1, pp. 85–89.

[8] Y. T. Su and L. D. Jeng, "Antijam capability analysis of RS-coded slow frequency hopped system," *IEEE Trans. Commun.*, vol. 48, no. 2, pp. 270–281, Feb. 2000.
[9] B. K. Levitt, "FH/MFSK performance in multitone jamming," *IEEE J. Sel. Areas Commun.*, vol. SAC-3, no. 5, pp. 627–643, Sep. 1985.
[10] P. J. Crepeau, "Performance of FH/BFSK with generalized fading in worst-case partial-band Gaussian interference," *IEEE J. Sel. Areas Commun.*, vol. 8, no. 5, pp. 884–886, Jun. 1990.
[11] Z. Yu, T. T. Tjhung, and C. C. Chai, "Independent multitone jamming of FH/MFSK in Rician channels," *IEEE Trans. Commun.*, vol. 49, no. 11, pp. 2006–2015, Nov. 2001.
[12] J. G. Proakis, *Digital Communications*. Singapore: McGraw-Hill, 2001.
[13] I. Gradshteyn and I. M. Ryzhik, *Handbook of Mathematical Functions*. London, U.K.: Academic, 1965.
[14] L. L. Yang and L. Hanzo, "A residue number system based parallel communication scheme using orthogonal signaling: Part II—Multipath fading channels," *IEEE Trans. Veh. Technol.*, vol. 51, no. 6, pp. 1547–1559, Nov. 2002.

General Exact Level Crossing Rate and Average Fade Duration for Dual-Diversity Combining of Nonidentical Correlated Weibull Signals

Daniel Benevides da Costa, *Student Member, IEEE*,
Michel Daoud Yacoub, *Member, IEEE*,
José Cândido Silveira Santos Filho,
and Gustavo Fraidenraich, *Member, IEEE*

***Abstract*—This paper derives general *exact* expressions for the level crossing rate (LCR) and the average fade duration (AFD) of dual-branch selection, equal-gain, and maximal-ratio combiners operating over nonidentical correlated Weibull fading channels. Sample numerical results are discussed by specializing the general expressions to a space-diversity system using horizontally spaced antennas at a mobile station. It is verified that as the antenna spacing becomes larger, the LCR decreases, becoming oscillatory and convergent. In addition, when the direction of the mobile is perpendicular to the axis of the antenna, the AFD is loosely dependent on the antenna spacing. Some simulation results are presented to verify the correctness of the analytical formulation.**

***Index Terms*—Average fade duration (AFD), diversity-combining techniques, level crossing rate (LCR), Weibull fading channels.**

I. Introduction

Diversity-combining techniques constitute an effective means to combat the deleterious effects of multipath fading on the performance of wireless communication systems. This performance can be evaluated by several measures, including the level crossing rate (LCR) and the average fade duration (AFD). Although the branch signals may be correlated and nonidentically distributed in practical systems [1]–[6], the literature on the LCR and AFD of diversity techniques over nonidentical correlated fading is not as rich as for the independent scenario. Pioneering work on this issue was carried out by Adachi *et al.* [1] for dual-branch selection combining (SC), equal-gain combining (EGC), and maximal-ratio combining (MRC) over balanced correlated Rayleigh channels. The unbalanced correlated Rayleigh and Ricean cases were addressed in [2] and [3] for MRC. In [4], Yang *et al.* presented a unified treatment for LCR and AFD of M-branch SC over unbalanced correlated Rayleigh, Ricean, and Nakagami-m channels. In [5], the LCR and AFD for the MRC were derived for a correlated unbalanced Nakagami-m environment. More recently, an extension of [1] for unbalanced channels was investigated in [6]. To the best of the authors' knowledge, these second-order statistics for correlated nonidentical Weibull fading channels have not been investigated in the literature yet. This paper derives general *exact* expressions for the LCR and AFD for dual-branch SC, EGC, and MRC combining systems in a Weibull fading environment. The expressions apply to nonidentical correlated diversity channels. Some numerical results are presented for a space-diversity system using horizontally spaced antennas at a mobile station. To verify the correctness of the analytical formulation, simulation data are also provided.

This paper is organized as follows: Section II establishes the model for the Weibull fading channels and derives the Weibull joint bidimensional envelope-phase density (JBEPD). Some key statistics involving the branch envelopes and their time derivatives are derived in Section III. Relying upon these statistics, general exact LCR and AFD expressions are also presented. Section IV computes the conditional means and variances for each diversity system. Section V shows some numerical and simulation plots, and Section VI draws some conclusions. Appendix A details the formulation of the complex covariance matrix. Appendix B demonstrates the relation between the conditional statistics (means, variances, and covariance) of the real variates with those of the complex variates.

II. Preliminaries

The Weibull distribution is an empirical distribution, which was first proposed aiming at applications in reliability engineering. It has also found use in wireless communications to model the fading envelope [7]–[9]. In [10] and [11], a very simple physical model for the Weibull distribution was proposed. In essence, in the proposed model, the received signal Z_i at branch i $(i = 1, 2)$ can be represented in a complex form as

$$Z_i = R_i^{\alpha_i/2} \exp(j\Theta_i) = X_i + jY_i \tag{1}$$

where $\sqrt{j} = -1$; R_i is the Weibull envelope; Θ_i is the Weibull phase, which is uniformly distributed in [0, 2π); X_i and Y_i are independent zero-mean Gaussian variates with identical variances σ_i^2; and $\alpha_i > 0$ stands for the Weibull fading parameter. The probability density function (pdf) $f_{R_i}(\cdot)$ of the envelope R_i is given by

$$f_{R_i}(r_i) = \frac{\alpha_i r_i^{\alpha_i - 1}}{\Omega_i} \exp\left(-\frac{r_i^{\alpha_i}}{\Omega_i}\right) \tag{2}$$

where $\Omega_i = \mathrm{E}(R_i^{\alpha_i}) = 2\sigma_i^2$, and $\mathrm{E}(\cdot)$ stands for the statistical average. For the special cases $\alpha_i = 1$ and $\alpha_i = 2$, (2) reduces to the

Manuscript received December 9, 2005; revised November 6, 2006, February 8, 2007, and February 12, 2007. This work was supported in part by FAPESP under Grant 05/59259-7. This paper was presented in part at the IEEE International Microwave and Optoelectronics Conference, Brasilia, Brazil, July 2005. The review of this paper was coordinated by Prof. Y. Ma.

D. B. da Costa, M. D. Yacoub, and J. C. S. Santos Filho are with the Wireless Technology Laboratory (WissTek), Department of Communications, School of Electrical and Computer Engineering, University of Campinas, Campinas 13083-852, Brazil (e-mail: daniel@wisstek.org; michel@wisstek.org; candido@wisstek.org).

G. Fraidenraich was with the Wireless Technology Laboratory (WissTek), Department of Communications, School of Electrical and Computer Engineering, University of Campinas, Campinas 13083-852, Brazil. He is now with the Department of Electrical Engineering, Stanford University, Stanford, CA 94305 USA (e-mail: gfraiden@stanford.edu).

Digital Object Identifier 10.1109/TVT.2007.901038